# Image Analysis Platform for Eye-Brain Interaction Research: Fundus Vascular Segmentation and Multi-Parameter Extraction Function

Haowei Kuang, Shiwei Luo, Huaitang Wang

*Southern University of Science and Technology*
*{11910710, 21990005, 11913005}@mail.sustech.edu.cn*

## Abstract

*In order to benefit the early diagnosis of Alzheimer's disease and considering the high correlation between the brain and the eye, we want to develop an image analysis platform for eye-brain linkage studies. Under the guidance of doctors in the group, we plan to implement a retinal vessel segmentation and parameter extraction function with accurate results, easy to use and fast computation under the framework of the eye-brain linkage platform, using OCTA images as the analysis object during this semester.*

## 1. Introduction

In this report, we develop an image analysis platformfor the study of eye-brain interaction, perform accurate segmentation and multi-parameter analysis of fundus blood flow, and deeply understand the correlation between fundus blood vessels and brain structure in AD, so as to assist in the early diagnosis of AD.

We try to choose histogram equalization method as our preprocessing method, using OCTA-NET algorithm as the vascular segmentation algorithm. After testing, our vascular segmentation algorithm plays a very good role. We also extracted multiple parameters from the segmented image, including vascular centerline, total length of vascular, vascular area, explants area, percentage of vascular area, fractal dimension and so on.. [1]

## 2. Related Work

### 2.1. IMED-ROSE dataset

iMED-ROSE is an OCTA dataset from iMED team[2]. It consists of two subsets: Rose- 1 and Rose-2. The subset ROSE-1 consisted of 117 OCTA images from 39 subjects (26 patients with disease and the rest healthy controls), divided into 90 images for training and 27 images for testing, including superficial (SVC), deep (DVC), and intraretinal vascular plexus. All OCTA scans were captured by the RTVue XR Avanti SD-OCT system (Optovue, USA) equipped with AngioVue software at a resolution of 304 × 304 pixels. The manual labeling of these vascular networks is scored by imaging experts and clinicians, and their consensus is taken as the basic fact. There are two different types of container annotations: centerline level annotations and pixel level annotations. The ROSE-2 subset contains 112 OCT-A images from 112 eyes. Ninety images were trained and 22 images tested. Each image is adjusted to a grayscale image of 840 × 840 pixels. All visible retinal blood vessels were manually tracked by experienced clinical ophthalmologists using software (Mathworks R2018,Natwick).

## 3. Data Preprocessing

After trying, we chose the histogram mean method as the pretreatment method of our experiment.The basic idea of equalization is to try to make the number of pixels in each gray level equal [1]. That is, there are no large swaths of similar pixels to improve the contrast of the image. The results are as follows: Figure 1 shows the result of applying histogram equalization to the OCTA image processing compared to the original image. Figure 2 shows the distribution of grayscale values of the rightmost image before and after processing.

The effect of histogram equalization: to make the image gray levels span a wider range of gray levels, thus improving the image contrast.

Another advantage of histogram equalization: no additional parameters are needed and the whole process is automatic.

The disadvantage of histogram equalization: some gray levels may not be mapped after stretching, resulting in a grainy image perception.

## 4. OCTA-Net

We use a split-based coarse-to-fine network, named as OCTA-Net, for retinal vessel segmentation in OCTA images. The pipeline of OCTA-Net has two indispensable stages - coarse stage and fine stage, as illustrated in Figure 3. In the coarse stage, a split-based coarse segmentation (SCS) module is used to produce preliminary confidence maps. In the fine stage, a split-based refined segmentation (SRS) module is used to fuse these vessel confidence maps to produce the final optimized results.

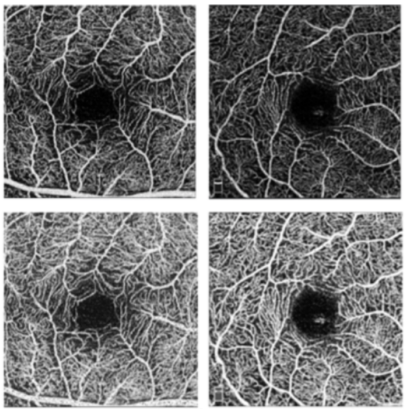

Figure 1. Histogram equalization(The top is the original image, and the bottom is the pre-processed image)

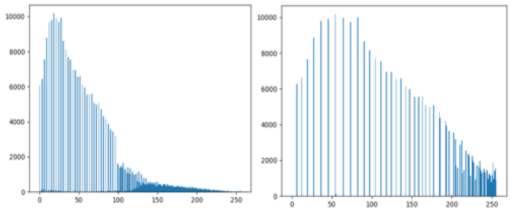

Figure 2. grey-scale distribution(Grayscale distribution before and after Histogram equalization)

### 4.1. Coarse Stage

Since the dataset has both pixel-level and centerline-level vessel annotations for each en face OCTA image, the split-based coarse segmentation (SCS) module has a partial shared encoder and two decoder branches (for pixel-level and centerline-level vessel segmentation, respectively), to balance the importance of both pixel-level and centerline-level vessel information, as illustrated in the coarse stage of Figure 3.

***1) Pixel-Level Vessel Segmentation:*** Pixel-level vessel segmentation is a U-shape network including five encoder layers and the symmetric decoder layers. A ResNet-style structure with split attention module, ResNeSt block [4], is used as the backbone of each encoder-decoder layer.

***2) Centerline-Level Vessel Segmentation:*** Compared with pixel-level annotation, vessel annotation at centerline level aims to grade the vessels in regions with poor contrast, more complex topological structures, and relatively smaller diameters. So the network structure is adjusted, several ResNeSt blocks followed by an up-sampling layer are appended in the third encoder layer of the backbone, as the decoder of the centerline-level vessel segmentation network.

### 4.2. Fine Stage

In order to further recover continuous details of small vessels, the fine stage is used to adaptively refine the vessel prediction results from the coarse stage. A split-based refined segmentation (SRS) module is used as the fine stage. The structure of SRS module is illustrated in the fine stage of Figure 3. In order to fully integrate pixel-level and centerline-level vessel information from the SCS module, the predicted pixel-level and centerline-level vessel maps and the original (single channel) OCTA image are first concatenated as input (total 3 channels) to the SRS module. In addition, the SRS module will produce adaptive propagation coefficients to refine the pixel-level and centerline-level maps respectively. Finally, the refined pixel- and centerline-level maps are then merged into a complete vessel segmentation map, by choosing the larger value from the two maps at each pixel.

## 5. Parametric Extraction

Vessels Area, Explant Area, Vessels Percentage Area, Total Vessels Length, Vessel Center Line, Fractal Dimension, Vessel Curvature.

### 5.1. Vessels Area

White part in Figure 4.

### 5.2. Explant Area

All valid areas in Figure 4.

### 5.3. Vessels Percentage Area

The ratio of vessels area and explant area.

### 5.4. Vessel Center Line

Use Rosenfeld refinement algorithm. Scan all pixels. If the pixel is a boundary point, but not an outliers and endpoints, and deletion of the pixel does not change the eight-connectivity of the surrounding eight pixels, delete the pixel. Repeat the scan until there are no pixels in the image that can be deleted. Then get the centerline image, as Figure 5.

### 5.5. Total Vessels Length

Calculated from the vessel center line.

### 5.6. Fractal Dimension

Fractal dimension expresses the internal regularity representation of the seemingly irregular shape of blood vessels. Since the box dimension is equal to the fractal dimension, we calculate the box dimension to get the fractal dimension.

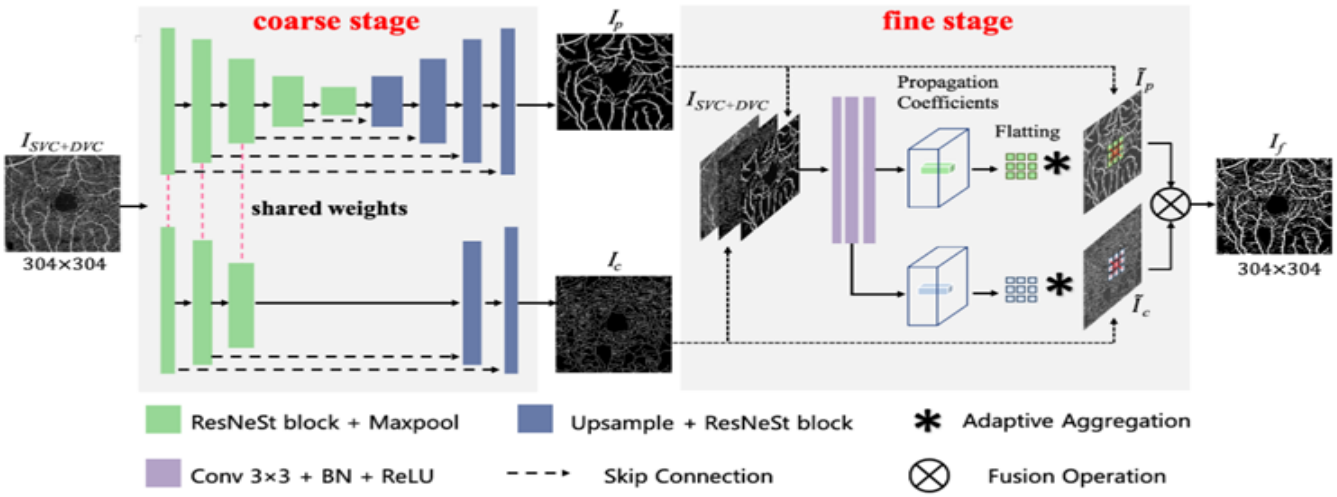


Figure 3. Architecture of the proposed OCTA-Net network (with an example of en face of the angioram of SVC+DVC in the ROSE-1 set). The SCS module (coarse stage) is designed to produce two preliminary confidence maps that segment pixel-level and centerline-level vessels, respectively. The SRS module (fine stage) is then introduced as a fusion network to obtain the final refined segmentation results.

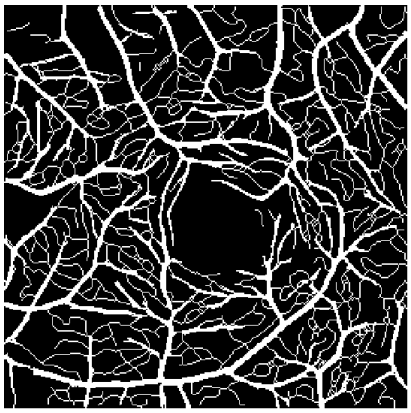

Figure 4. Vessels Segmentation Vessels Area(white area)

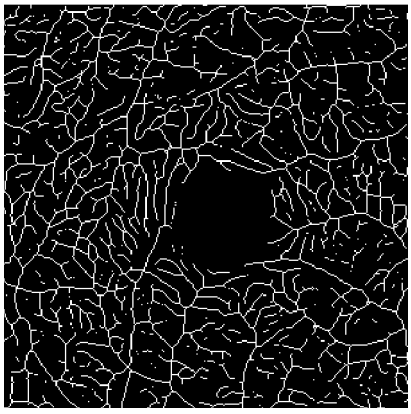

Figure 5. Vessel Center Line

We place the blood vessels on a evenly divided grid and calculate the minimum number of cells needed to cover the blood vessels. By progressively refining the grid, the change in the number of coverage required is viewed to calculate the box dimension. The calculation formula is as $dim_{box}(S) = \lim_{\epsilon \to 0} \frac{\log N(\epsilon)}{\log (1/\epsilon)}$ Figure 6.

Figure 6. Fractal Dimension ( $\epsilon$ represents the side length of the lattice and N represents the number of cells required to cover the vessels).

## 5.7. Vessel Curvature

Curvature convolution kernel is used to extract the curvature of segmented vascular images. Firstly, the algorithm performs open operation on the segmented image, that is first corrodes and then expands. Secondly, perform closed operation, that is first expands and then corrodes. Finally, the curvature of the image is calculated according to the formula as $H = \begin{bmatrix} -\frac{1}{16} & \frac{5}{16} & -\frac{1}{16} \\ \frac{5}{16} & -1 & \frac{5}{16} \\ -\frac{1}{16} & \frac{5}{16} & -\frac{1}{16} \end{bmatrix} \otimes U$ Figure 7.

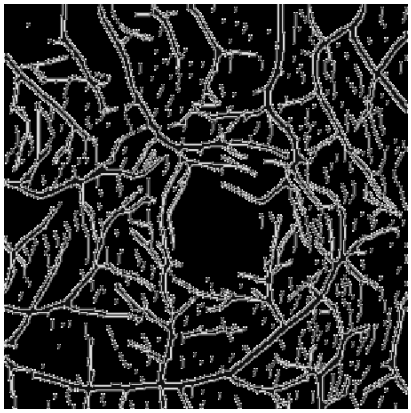

Figure 7. Vessel Curvature Formula 6.12 of [7]

# 6. Experiments

## 6.1. Experimental Setting

The proposed method was implemented with PyTorch. Both the coarse and the fine stage were trained with 300 epochs and with the following settings: Adam optimization with the initial learning rate of 0.0005, batch size of 2 and weight decay of 0.0001. For more stable training, we adopted poly learning rate policy with a poly power of 0.9. For training and inference of the proposed method, the ROSE [5] subset was split into 30 images for training and 9 images for testing. Data augmentation was conducted by randomly rotation of an angle from -10° to 10°during all training stages.

## 6.2. Evaluation Metrics

To achieve comprehensive and objective assessment of the segmentation performance of the proposed method, the following metrics are calculated and compared:

- Area Under the ROC Curve (AUC)
- Sensitivity (SEN)=TP/(TP+FN)
- Specificity(Specificity)=TN/(TN+FP)
- Accuracy(ACC)=(TP+TN)/(TP+TN+FP+FN)
- Kappa score=$(Accuracy - p_e)/(1 - p_e)$
- False Discovery Rate(FDR) = FP/(FP + TP)
- G-mean score [6]=$\sqrt{Sensitivity \times Specificity}$
- Dice coefficient(Dice)=2×TP/(FP+FN+2×TP)

where TP is true positive, FP is false positive, TN is true negative, and FN is false negative. pe in Kappa score represents opportunity consistency between the ground truth and prediction, and it is denoted as:
$p_e = ((TP + FN)(TP + FP) + (TN + FP)(TN + FN))/(TP + TN + FP + FN)^2$

## 6.3. Performance Comparison and Analysis

We compared the effects of different pretreatment methods on the segmentation results on ROSE dataset and evaluated the segmentation accuracy of the proposed algorithm. Then, we also test the portability of the segmentation algorithm on iMED-Huaxi dataset to prove that the algorithm has good portability and can be used in our platform development.

## 6.4. Segmentation Accuracy Comparisons

In order to compare and obtain the most suitable preprocessing methods, we carried out four different preprocessing methods for images, including histogram equalization method, top hat transformation method, CLAHE method and gamma transformation method. The model was trained on the training set and evaluated on the test set respectively, and the results were as follows.

From Table 1, We can see that through the improvement of the training method, the results of the model trained by us are significantly improved compared with the results in the paper. After comparing and analyzing the results of four kinds of pretreatment, we finally choose histogram averaging method as our pretreatment method.

## 6.5. Portability Test

Then, we verify the portability of the model on iMED-Huaxi dataset. We used two types of images of superficial vessels and deep vessels to verify the mobility of the model. Since this dataset was not manually annotated, we evaluated the segmentation results under the guidance of clinicians. The following Figure 8. shows the segmentation results of the original images of superficial vascular data and deep vascular data and our model.

After staining observation, we found that our model performed well on both types of images on the dataset both in overall and in detail. It is proved that our model has good transferability.

So we can come to the conclusion. The vascular segmentation algorithm we implemented has been tested and has good segmentation accuracy and portability, which can be used in the development of vascular extraction and analysis platform functions.

# 7. Platform

We finally succeeded in building a medical image processing platform with easy operation. The platform can be used for processing OCTA images, allowing for vessel

TABLE 1. SEGMENTATION RESULTS OF ORIGINAL IMAGES AND IMAGES OBTAINED BY DIFFERENT PRETREATMENT METHODS ON ROSE

| Method | AUC | ACC | FDR | Kappa | G-mean | Dice |
|---|---|---|---|---|---|---|
| Thesis results | 0.945 | 0.918 | 0.178 | 0.720 | 0.836 | 0.770 |
| original image | 0.949 | 0.921 | 0.146 | 0.728 | 0.832 | 0.775 |
| Histogram equalization | 0.950 | 0.922 | 0.142 | 0.725 | 0.828 | 0.771 |
| Top-Hat | 0.933 | 0.917 | 0.121 | 0.697 | 0.797 | 0.745 |
| CLAHE | 0.950 | 0.922 | 0.104 | 0.716 | 0.807 | 0.761 |
| Gamma transform | 0.950 | 0.923 | 0.120 | 0.725 | 0.820 | 0.770 |

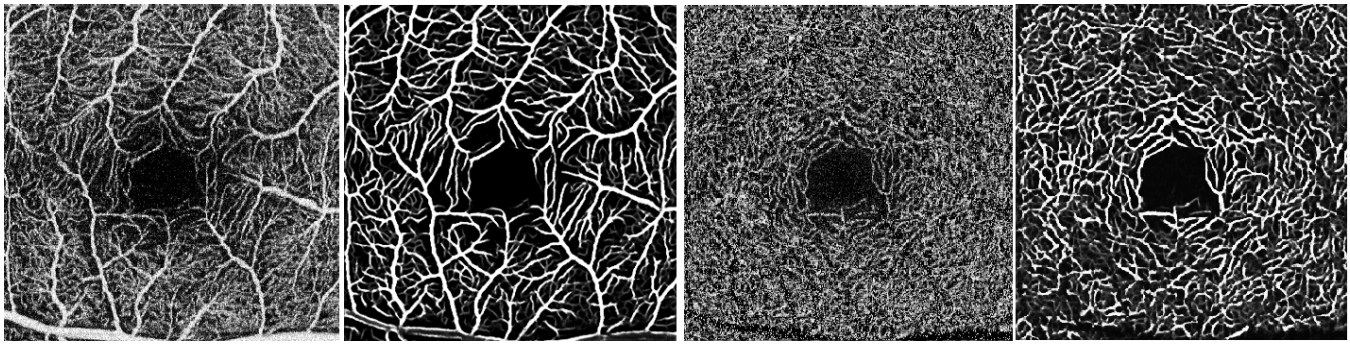

Figure 8. OCTA image and segmentation results. From left to right: images of shallow vessels, segmentation results of shallow vessels, images of deep vessels, segmentation results of deep vessels

segmentation, browsing and management of datasets, as well as manual annotation, multi-parameter extraction. The name of the platform is ELIA, Figure 9.

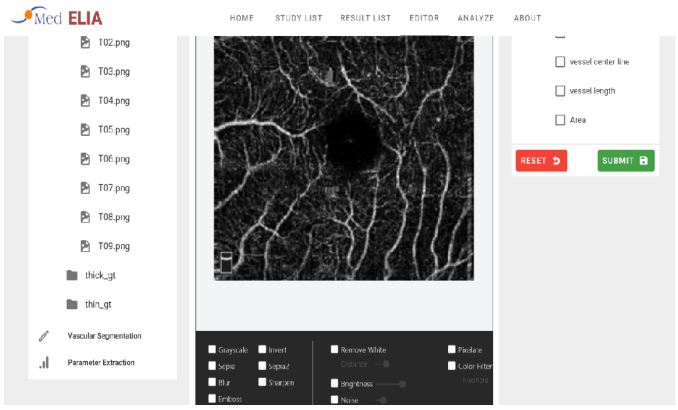


Figure 9. ELIA

## 8. Conclusion

In this semester's work, we developed an image analysis platform for the study of eye-brain linkage. We conducted repeated model training for the OCTA-NET method of vessel segmentation and OCTA vessel image extraction, and improved the quality of the model by adjusting the training method and adding the pretreatment method, thus realizing the function of vessel segmentation. In addition, we also tested the segmentation method on multiple data sets to verify the portability of the method. We have also developed multi-parameter extraction capabilities for blood vessels and integrated them into a platform that clinicians can use easily. The professionalism and accuracy of our functions and the convenience of our platform have been recognized by professional doctors.

## 9. Acknowledgement

In the end, we would like to express our special thanks to Professor Jin Zhang and Professor Jiang Liu for their guidance and help throughout our project. In addition, we would like to thank Senior sister Hanpei Miao, Senior brother Zhongxi Qiu and Senior Brother Richu Jin for their great help to our project. Without them, our project would not have been completed.

# References


[1] Z. Zhang, H. Zhang, and Z. Pei, "Adaptive equalization algorithm for image based on histogram," in *2014 International Conference on Mechatronics, Electronic, Industrial and Control Engineering (MEIC-14)*. Atlantis Press, 2014, pp. 1298–1301.

[2] X. Bai, F. Zhou, and B. Xue, "Image enhancement using multi scale image features extracted by top-hat transform," *Optics & Laser Technology*, vol. 44, no. 2, pp. 328–336, 2012.

[3] S.-C. Huang, F.-C. Cheng, and Y.-S. Chiu, "Efficient contrast enhancement using adaptive gamma correction with weighting distribution," *IEEE transactions on image processing*, vol. 22, no. 3, pp. 1032–1041, 2012.

[4] H. Zhang, C. Wu, Z. Zhang, Y. Zhu, H. Lin, Z. Zhang, Y. Sun, T. He, J. Mueller, R. Manmatha *et al.*, "Resnest: Split-attention networks," *arXiv preprint arXiv:2004.08955*, 2020.

[5] Y. Ma, H. Hao, J. Xie, H. Fu, J. Zhang, J. Yang, Z. Wang, J. Liu, Y. Zheng, and Y. Zhao, "Rose: a retinal oct-angiography vessel segmentation dataset and new model," *IEEE transactions on medical imaging*, vol. 40, no. 3, pp. 928–939, 2020.

[6] J.-H. Ri, G. Tian, Y. Liu, W.-h. Xu, and J.-g. Lou, "Extreme learning machine with hybrid cost function of g-mean and probability for imbalance learning," *International Journal of Machine Learning and Cybernetics*, vol. 11, no. 9, pp. 2007–2020, 2020.

[7] Y. Gong, "Spectrally regularized surfaces," Ph.D. dissertation, ETH Zurich, 2015.